Food Chemistry 424 (2023) 136385

Contents lists available at ScienceDirect

Food Chemistry

journal homepage: www.elsevier.com/locate/foodchem

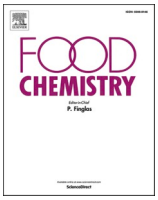

All-natural wheat gliadin-gum arabic nanocarriers for encapsulation and delivery of grape by-products phenolics obtained through different extraction procedures

Serena Carpentieri [a], Giovanna Ferrari [a,b], Francesco Donsì [a,*]

[a] Department of Industrial Engineering, University of Salerno, Via Giovanni Paolo II, 132, 84084 Fisciano, SA, Italy
[b] ProdAl Scarl c/o University of Salerno, Via Giovanni Paolo II, 132, 84084 Fisciano, SA, Italy

ARTICLE INFO

Keywords:
Grape pomace
Extraction
Colloidal systems
Anti-solvent precipitation
Bioaccessibility
Simulated digestion

ABSTRACT

Grape pomace (GP), the major winery by-product, is still rich in phenolic compounds, scarcely applied in food systems due to physicochemical instability issues. This work aimed at fabricating gliadin (G)-based nanoparticles through antisolvent precipitation, for delivery of GP extracts, investigating different extraction strategies with ethanol/water solution (70:30 v/v). Interestingly, the fabricated nanoparticles were characterized by a nanometric size range with hydraulic diameter values around 100 nm and ζ-potential of 18–22 mV. The addition of gum arabic (GA), at the optimized G/GA ratio 1:1, improved particle stability and encapsulation efficiency of GP polyphenols. The two-step extraction of GP in the G-rich solvent retrieved from G extraction, as evidenced by total phenolics (1.24 times higher than the two separately obtained extracts G/GP10:10), HPLC-PDA analysis, encapsulation efficiency (62.9% in terms of epicatechin), and simulated digestion (95.6% release of epicatechin), represented the most promising approach to obtain G nanoparticles for efficient delivery of GP extracts.

1. Introduction

Nowadays, the food industry is continuously struggling to introduce on the market natural products to satisfy the growing consumers' demand, and, at the same time, is seeking to adopt sustainable production strategies in line with the 17 sustainable development goals adopted by the United Nations Member States (Carpentieri, Larrea-Wachtendorff, Donsì, & Ferrari, 2022b).

For these reasons, the global natural extracts market, driven by an increasing change in the consumers' lifestyle and awareness, biotechnological advancements, and overall health benefits associated with the incorporation in food of natural extracts, is expected to double by 2030 (Precedence Research, 2022). In this frame, agri-food by-products, which are still rich in healthy compounds, such as fiber, polyphenols, protein, fatty acids, vitamins, and minerals, represent an affordable and widely available source of bioactive compounds (BACs), which can be exploited as food ingredients to promote human health (Carpentieri et al., 2022b).

Winemaking, which is one of the most widespread agricultural activities worldwide, produces large amounts of grape pomace (GP), the major winery by-product (between 10% and 30% of the total processed grape), whose management and disposal have relevant environmental impacts. It is estimated that 1 kg of GP is generated from 6 L of wine production (Carpentieri, Ferrari, & Pataro, 2022a).

GP has been recognized as an important source of BACs, such as polyphenols, which, after winemaking, remain in pomace for up to 70% of their initial content in grapes. Polyphenols represent an important class of BACs, not only used in the food industry but also in the pharmaceutical, cosmetic, packaging, and textile industry, thanks to their antioxidant, antimicrobial, and coloring properties, among others (Albuquerque and Heleno, 2021). Although it is difficult to uniquely define the polyphenols composition of GP due to the strong variability between grape varieties and winemaking processes, several studies reported that the major phenolic compounds of winery by-products, comprising flavonoids (flavanols or flavan-3-ols, proanthocyanidins, flavones, and flavonols), phenolic acids (hydroxybenzoic acids and hydroxycinnamic acids), and stilbenes, have been reported as responsible for multiple health beneficial effects (Costa et al., 2021). However, the physicochemical instability of phenolic compounds and their low delivery efficiency toward target sites limit their applications in complex food systems (Li et al., 2021).

To this purpose, coherently with the need for cost-effective and

* Corresponding author.
E-mail address: fdonsi@unisa.it (F. Donsì).

https://doi.org/10.1016/j.foodchem.2023.136385
Received 1 December 2022; Received in revised form 21 March 2023; Accepted 13 May 2023
Available online 24 May 2023

clean-label products, natural-based colloidal particles have been proposed as generally regarded as safe (GRAS) delivery systems for their encapsulation, protection, and release (Yang et al., 2021).

The usage of biodegradable polymeric nanoparticles has attracted the interest of many research groups in the food and pharmaceutical fields, due to their favorable properties, such as good biocompatibility and adaptability, easy design and preparation, interesting bio-mimetic features and high binding affinities with BACs, able to protect them from oxidation and enzymatic hydrolysis (Su et al., 2021). The use of plant proteins such as soy protein, zein, and gliadin, is presently viewed as a "green" trend because they are recognized to be less allergenic than animal proteins, cost-effective, and readily available (Wu et al., 2018).

Wheat gliadin (G) is the major storage protein of wheat and has a good ability to spontaneously form colloidal structures in the aqueous phase, suitable for delivering bioactive compounds due to its amphiphilic properties and self-assembly capability. It is water-insoluble but soluble in an aqueous solution at 70 % (v/v) of ethanol (Su et al., 2021), and this property makes G a proper material for all-natural delivery systems especially compatible with wheat-based products.

However, G nanoparticles prepared by liquid antisolvent (LAS) precipitation are sensitive to the stresses induced by pH and heating, leading to the formation of aggregates and instability (Wu et al., 2018). Several studies have recently shown that protein-polysaccharide interactions can enhance the stability of protein nanoparticles. Many polysaccharides have been demonstrated to be good stabilizers for G-based nanoparticles used as delivery carriers for nutraceuticals, including casein (Wu et al., 2022), sodium alginate (Su et al., 2021), chitosan (Yang et al., 2021; Zeng et al., 2019), sodium carboxymethyl cellulose (He et al., 2022), rhamnolipid composite (Chen et al., 2021).

Among the polysaccharides, gum arabic (GA), an edible dried gummy exudate from the stems of Acacia senegal and Acacia seyal, also found as color preservative and non-enzymatic browning inhibitor, due to its prebiotic effect, digestive tolerance, higher soluble fiber content and water solubility, lower viscosity and caloric value than other polysaccharides, (Williams and Phillips, 2021; Wu et al., 2018), is the most commonly used as encapsulating agent to stabilize several proteins, including zein (Gali et al., 2022), and wheat G nanoparticles (Wu et al., 2018, 2020). Its characteristics are mainly attributed to the branched structure of GA giving rise to compact molecules with a relatively small hydrodynamic volume compared to that much larger of other polysaccharides characterized by linear molecules (e.g. xanthan gum, sodium carboxymethyl cellulose) promoting the formation of intermolecular entanglements (Williams and Phillips, 2021).

Previous studies on the fabrication of G colloidal particles as vehicles for bioactive compounds focused on the encapsulation of pure compounds, such as curcumin (Chen et al., 2021; Su et al., 2021; Yang et al., 2021; Zeng et al., 2019; Zhang et al., 2022), natamycin (Wu et al., 2022), phloretin (He et al., 2022), and resveratrol (Wu et al., 2020). None of them focused on the direct encapsulation of extracts with complex composition, nor of extracts recovered from agri-food residues, which can be expected to be challenging in terms of control of the particle size of G particles and encapsulation efficiency, due to the complex composition of the extracts and unpredictable interaction with the polymeric matrix (Gali et al., 2022). In addition, previous studies on the encapsulation of BACs in G-based delivery systems have mostly used, as an encapsulating agent, commercial G (Wu et al., 2022; Zeng et al., 2019; Zhang et al., 2022) or G extracted from commercial gluten (Chen et al., 2021; He et al., 2022; Su et al., 2021; Wu et al., 2020; Yang et al., 2021), rather than G extracted directly from wheat semolina. Extracting G from wheat semolina is a challenging step because a likely less pure G is obtained, but, at the same time, it is a fundamental step towards a more sustainable production process of G-based delivery systems.

This study aims at developing a facile and versatile two-step combined approach, involving the extraction of different phenolic compounds from red GP and the extraction of G from durum wheat semolina, for the direct entrapment of the GP extract, through antisolvent precipitation, in G-based colloidal particles.

Additionally, the potential synergistic effects of different extraction procedures, involving also a one-pot process for the concurrent extraction of bioactive compounds from GP and of G from semolina on the extraction efficiency and subsequent formation of colloidal particles with and without the addition of GA as a natural stabilizing agent are also studied.

Finally, the effect of the different extraction procedures on the composition of the GP extracts, as well as on the encapsulation efficiency and release during simulated digestion for both G- or G/GA-based formulations is also investigated.

2. Materials and methods

2.1. Raw materials and chemicals

Fresh red grape pomace (GP) of the "Aglianico" variety, mainly composed of skins and seeds, with a moisture content on wet basis of 66.3 ± 0.3%, was provided by a local winery (Sabino Urciuoli S.a.s, Atripalda (AV), Italy). Samples were collected during the winemaking process and stored frozen (T = − 20 °C) until use. Durum wheat semolina was provided by a local pasta producer company and stored in sealed BOPP bags until use.

Gluten from wheat (CAS number: 8002–80-0), gum arabic from acacia (CAS number: 9000–01-5), ethanol, α-amylase (A3176, ≥ 5 U/mg) from porcine pancreas, pepsin (P7000, 674 U/mg) from porcine gastric mucosa, pancreatin (P3292, 4 × USP) from porcine pancreas, bile salts (B8756), and all the chemicals and reagents involved in the analyses were purchased from Sigma Aldrich (Steinheim, Germany).

2.1.1. Proximate composition of durum wheat semolina

AOAC (2005) methods were employed for the analysis of moisture content (AOAC 925.10), protein content (micro-Kjeldahl method AOAC 920.87, with a factor of 5.7 used to convert the nitrogen to protein content), ash content (AOAC 923.03), fat content (AOAC 922.06). Total dietary fiber was determined by a commercial kit (Megazyme K-TS, Wicklow, Irlanda) according to the method AACC 32–05.01 and AOAC 985.29. The extraction of gluten was carried out manually using a solution of monosodium phosphate and disodium phosphate, following the method described by Tateo (1980). Total starch (TS) content was determined by a commercial kit (Amyloglucosidase/α-Amylase Method, Megazyme K-TS, Wicklow, Irlanda) according to AOAC Method 996.11 and AACC Method 76–13.01. The amylose content of semolina samples was determined according to the official method K-Amyl 06/18.

All analyses were performed in triplicate, and the results were reported on a dry-weight basis.

2.2. Preparation of hydroalcoholic extracts

GP (10% w/v) was extracted at previously optimized extraction conditions, by maceration in an ethanol/water solution (70:30 v/v) under continuous stirring (200 rpm), for 5 h, at 50 °C. G was extracted from (i) wheat gluten (DG), previously recovered from semolina (see section 2.1.1), (ii) commercial gluten (CG), and (iii) directly from durum wheat semolina (S), according to the method described by Wu et al. (2018), with slight modifications. Briefly, DG (10% w/v), CG (10% w/v), and S (50% w/v) were dissolved in an ethanol/water solution (70:30 v/v) for 5 h at 50 °C, followed by centrifugation at 6500 rpm for 20 min to remove insoluble impurities. The different extracted G solutions were analyzed in terms of total protein content (Section 2.1.1) and subjected to SDS-Page for protein identification (Section 2.2.1).

Likewise, the co-extract (S and GP are extracted concurrently with the ethanol/water solution at 70:30 v/v, in a one-pot extraction step), and the two-step extracts S + GP (the same ethanol/water solution at 70:30 v/v is used sequentially to extract first S and then, once enriched in G, to extract BACs from GP) and GP + S (the same ethanol/water

solution at 70:30 v/v is used to first extract GP and then, once enriched in GP extracts, to extract G from S) were obtained by following the same extraction conditions previously described. It can be expected that different extraction strategies might affect the yield of extraction, by changing the affinity of the second extract for the enriched solvent, and the encapsulation efficiency by affecting the molecular interactions in the solvent. Figure S1, reported in the Supplementary material, helps the reader to better understand the performed extraction procedures, by providing a schematization of the steps involved in the different extraction processes.

2.2.1. SDS-PAGE

SDS-PAGE electrophoresis was carried out as described by Carullo et al., 2021 with slight modifications. Briefly, the samples were diluted in a Tris-HCl buffer (0.125 mol/L, pH = 6.8) containing SDS (2% w/w), glycerol (10% w/w), bromophenol blue (0.02% w/w) and β-mercaptoethanol (5% w/w) as a reducing agent. Separating (12%) and stacking (6%) polyacrylamide gels were added with 50 μL of ammonium persulfate solution (10% w/v) and 5 μL of N, N, N′, N′-tetra methylethylenediamine (TEMED). 6 μL of all samples (DG, CG, S) were loaded into the prepared gels, together with a pre-stained Protein Marker (peqGOLD, 10–260 kDa), and run at constant voltage (100 V) for 2 h. The gels were then recovered and stained with a staining solution (0.1% Coomassie Brilliant Blue R 250, 10% acetic acid, 20% isopropanol) overnight. A de-staining solution (30% methanol, 10% acetic acid) was used to bleach the background.

2.3. G and G/GA particles fabrication

Gum arabic (GA) was selected to further improve the stability of G nanoparticles. The nanoprecipitation method was used to form G or G/GA colloidal particles in suspension (Gali et al., 2022). GA solution was prepared in ultrapure water at different concentrations under magnetic stirring for 5 h and stocked overnight at ambient temperature.

A volume of 20 mL of G hydroalcoholic solution was added dropwise to 100 mL of ultrapure water, to obtain G particles, or to a GA solution at different concentrations (G/GA ratios of 10:1, 5:1, 2:1, 1:1, 1:5, and 1:10 wt), to obtain G/GA particles, under continuous stirring (400 rpm) and the mixture was left for 30 min under stirring. A suspension of GA in water (1.25% wt) was also prepared as a control. Samples were subjected to ethanol removal under reduced pressure at 30 °C using a rotary evaporator (BÜCHI Labortechnik AG, R-300, Flawil, Switzerland). The eliminated volume (about 50% of the initial volume) was replaced by ultrapure water.

2.4. GP-rich particles fabrication

Different volumes of GP extract in hydroalcoholic solution (70:30 v/v) were brought, through the addition of a stock hydroalcoholic solution at the same concentration, to 10 mL and then mixed with a 10 mL of G hydroalcoholic solution, recovered from durum wheat semolina, to obtain different mass ratios of G/GP (10:2, 10:4, 10:6, 10:8, 10:10 v/v). The resulting solutions were then added dropwise to 100 mL of ultrapure water under magnetic stirring (400 rpm) at room temperature for 30 min. G:GP at mass ratios of 10:0 (blank G nanoparticles) and 0:10 (unencapsulated extract) were also prepared for sake of comparison. From the optimal conditions obtained for the GP extract and G recovered separately (G:GP ratio of 10:10 v/v), also the co-extract and the sequential extracts S + GP and GP + S were obtained and precipitated through LAS by addition dropwise to ultrapure water or GA aqueous solution (G:GA 1:1 wt) under magnetic stirring (400 rpm) at room temperature for 30 min.

A schematic representation of the fabrication of both GP- rich particles and G/GA particles is depicted in Figure S2 of the Supplementary material.

2.5. Spectroscopic analysis

UV/visible spectra of the samples in ethanol/water solution, hence before precipitation, were determined using a UV/ visible spectrophotometer (V-650, Jasco Inc. Easton, MD, USA) with a scanning range of 200–600 nm and a scan speed of 1000 nm/min, using ethanol/water solution (70:30, v/v) as a blank for the different extraction strategies.

2.6. Determination of hydrodynamic diameter, polydispersity index, ζ-potential, and pH

The hydrodynamic diameter (dH), the polydispersity index (PdI), and the ζ-potential of the colloidal particles were measured by dynamic light scattering (DLS) and electrophoretic mobility using a Zetasizer Nano ZS90 (Malvern Instruments, Ltd., Malvern, UK). The pH was determined using a pH-meter BASIC 20+ (Crison Instrument, Barcelona, Spain). All measurements were carried out in triplicate at 25 °C.

2.7. High-Performance Liquid-Chromatography analysis

A Waters 1525 Separation Module coupled to a photodiode array detector Waters 2996 (Waters Corporation, Milford, MA, USA) was used to perform the high-performance liquid chromatography–photodiode array detection (HPLC–PDA) analysis for the identification of phenolic compounds in the extracts, according to the method reported by Carpentieri, Ferrari, et al. (2022). The separation of the identified compounds was carried out in a Waters Spherisorb C18 reverse-phase column (5 μm ODS2, 4.6 × 250 mm, Waters Corporation, Milford, MA, USA). The extracts were first dried using a rotary evaporator and then dissolved in methanol, filtered with a 0.45 μm filter, and injected into the column (injection volume 5 μL). The mobile phase, with a flow rate of 0.8 mL/min, was composed of phosphoric acid (0.1%, eluent A) and methanol (100%, eluent B). The elution conditions were set as follows: 0–30 min from 5% B to 80% B, 30–33 min 80% B, and 33–35 min from 80% B to 5% B. The signal for the quantification of each compound was reported at the wavelength of maximum absorbance λ = 320 nm, 280 nm, 283 nm, and 260 nm for chlorogenic acid and p-coumaric acid, epicatechin, naringin, and rutin, respectively. The retention times of the identified compounds were compared with those of commercial standards and the results were reported as mg/g_{DW} of GP.

2.8. Encapsulation efficiency

The encapsulation efficiency (EE) for total phenolic compounds (TPC) and antioxidant activity of the different formulations was determined using the Folin-Ciocalteu method and Ferric Reducing Antioxidant Activity assay (FRAP), respectively, as previously reported by Carpentieri, Ferrari, et al. (2022). Samples were centrifuged at 14000 rpm for 20 min in an Eppendorf centrifuge (Micro Centrifuge 5417R, Eppendorf Srl, Milan, Italy). For the TPC determination, 0.5 mL of extract was mixed with 2.5 mL of 10% (v/v) Folin-Ciocalteau reagent and then added with 2 mL of sodium carbonate (7.5%, w/v). The absorbance of the mixture was measured at 765 nm after incubation for 1 h at room temperature in the dark, using a UV/Vis spectrophotometer (V-650, Jasco Inc. Easton, MD, USA). A calibration curve using gallic acid as the standard was used. The antioxidant activity was assessed by FRAP assay: 2.5 mL of freshly prepared FRAP working solution and 0.5 mL of extract were mixed and incubated for 10 min at ambient temperature. The absorbance of the mixture was then measured at 593 nm with the UV/Vis spectrophotometer. Ascorbic acid was used for the external standard calibration curve in a concentration range comprised between 0 and 2.0 mmol/L. EE was determined by the following formula (Eq. (1)):

$$EE(\%) = \frac{Total\ loaded\ extract - Free\ extract}{Total\ loaded\ extract} \times 100 \quad (1)$$

where *Total loaded extract* and *Free extract* are the values of TPC or antioxidant activity measured in the extracts before encapsulation and in the supernatant after encapsulation, respectively. For the calculation of EE (%) in terms of both TPC and antioxidant activity of GP extracts, the contributions of GA and G in each investigated suspension were subtracted from the total antioxidant activity and TPC of the whole systems.

The same procedure was followed for determining the encapsulation efficiency for the main identified phenolic compounds quantified by HPLC-PDA analysis (Section 2.7) in the extracts before encapsulation and in the supernatant.

2.9. Simulated gastrointestinal digestion

The simulated gastrointestinal digestion was assessed on selected systems stabilized or not by GA (G/GP = 0:10 v/v, G/GP = 10:10 v/v, S + GP, GP + S), following the international consensus procedure described by Minekus et al. (2014), with slight modifications. Briefly, 20 mL of the freshly prepared colloidal suspensions were mixed with an equal volume of simulated salivary fluid (SSF), consisting of 5 g/L of α-amylase, 0.117 g/L of NaCl, 0.149 g/L of KCl, 2.1 g/L of $NaHCO_3$, and 0.074 g/L of $CaCO_3$. After the oral phase, 40 mL of the oral bolus was mixed with 40 mL of the simulated gastric fluid (SGF), consisting of pepsin solution (3.2 g/L), 2 g/L of NaCl, and 7% (v/v) HCl 37%. Then, the mixture was adjusted to pH 3 with 1 M HCl and incubated at 37 °C for 120 min under continuous stirring at 130 rpm. After the gastric phase, 80 mL of the gastric digesta was mixed with 80 mL of the simulated intestinal fluid (SIF) consisting of 5 g/L of pancreatin, 0.2 g/L of $CaCO_3$, 0.2 g/L of CaCl, 1.75 g/L of NaCl, and 25 g/L of bile salts. The pH was adjusted to a final value of 7 by the addition of HCl (0.1 M) and NaOH (0.05 M) and incubated at 37 °C for 120 min under continuous stirring at 130 rpm. Samples, which were withdrawn after the oral phase, after 60 and 120 min of gastric phase, 20 and 120 min of intestinal phase, were centrifuged at 14000 rpm at 4 °C for 20 min using an Eppendorf centrifuge (Micro Centrifuge 5417R, Eppendorf Srl, Milan, Italy). TPC release from the nanoparticles was determined as described in Section 2.8. The release of epicatechin was monitored by HPLC, as described in section 2.7, and the percentage of release was calculated as reported by Gali et al. (2022).

2.10. Statistical analysis

All the experiments and analyses were performed in triplicate and the results were reported as means ± standard deviations. Differences among mean values were analyzed by one-way variance (ANOVA) using SPSS 20 (SPSS IBM, Chicago, USA) statistical package. Tukey test was carried out to determine statistically significant differences ($p < 0.05$).

3. Results and discussion

3.1. Wheat gliadin extraction and characterization

Durum wheat semolina is mainly composed of proteins (12–15% dry weight (dw)) and starch (74–76% dw) (Garcia-Valle et al., 2021) consisting of amylopectin and amylose in a 3:1 ratio (Lafiandra et al., 2022). High protein and gluten content (>11% dw, accounting for 60–85% of the total proteins) are decisive characteristics of high-quality semolina (Horvat et al., 2021). The semolina utilized in this study was characterized by a moisture content of 14.3 ± 0.94 % (w/w), a fat content of 0.86 ± 0.05 % (w/w), a content of total dietary fibers of 4.5 ± 0.11 % (w/w), and ash content of 0.6 ± 0.04 % (w/w), in good agreement with previous findings (Padalino et al., 2015). The detected protein and starch contents were 13.3 ± 0.54 % (w/w), and 66.4 ± 2.0 % (w/w), respectively, with 19.4 ± 0.8 % (w/w) of starch consisting of amylose. Moreover, the extraction yield of gluten from durum wheat semolina was 11.3 ± 0.5% (dw), representing 85% of the total protein content. These values are aligned with the data reported in previous studies (Horvat et al., 2021), as above mentioned, confirming the high standard quality of the durum wheat semolina.

Durum wheat proteins, based on their solubility, are classified as albumins (soluble in water), globulins (soluble in diluted saline), gliadins (soluble in 60–70% alcohol), and glutenins (soluble in diluted acid and alkali) (Shewry, 2019).

G represents around 40%-50% of total wheat storage proteins (Rani et al., 2022), corresponding to 4.5–8 g/100 g of semolina (dw). Interestingly, from the extraction process by using ethanol–water 70% (v/v), 38 ± 2.7 g of gliadin/100 g of CG (dw), 5.0 ± 0.7 g of gliadin/100 g of semolina (dw) and 3.4 ± 0.6 of gliadin/100 g of semolina (dw) were obtained directly from commercial gluten (CG), durum wheat semolina (S) and gluten previously recovered from the semolina (DG), respectively. Therefore, the obtained results demonstrated that almost all the G can be efficiently recovered directly from semolina in a one-pot extraction step, avoiding the time-consuming gluten extraction step.

3.1.1. SDS-PAGE of gliadin proteins

Gliadins, belonging to the monomeric prolamin fraction, are classified into three groups of polypeptides (α/β-, γ- and ω-gliadins) according to their molecular weight and electrophoretic mobility (Horvat et al., 2021).

The obtained electrophoretic gel of the extracts obtained from different sources (S, DG, and CG) is shown in Fig. 1.

Molecular weight (MW) bands were detected between 20 and 120 kDa, for all the extracts investigated. Thus, the extracted G included the medium molecular weight (MMW) fraction containing ω-gliadin monomers and low molecular weight (LMW) fraction comprised of α/β-gliadins, and γ-gliadins (Žilić et al., 2011). From the SDS-PAGE patterns, the extracts were found to be enriched in α- and β-gliadins while slightly depleted of the other protein fractions. In particular, the characteristic bands were observed at the corresponding MW ranges of 95–75 kDa for ω-gliadins, 60–50 kDa for γ-gliadins, 50–37 kDa for α- and β-gliadins.

Unless slight variations occur due to different extraction methods and wheat cultivars, these results are in agreement with previous findings, which reported for hydroalcoholic G extracts an average MW ranges of 52–100 kDa, 41–60 kDa, and 25–41 kDa, for ω-gliadin, γ-gliadin, and α-, β-gliadin, respectively (Rani et al., 2022; Schalk et al., 2017). Moreover, the MW ranging from 10 to 20 kDa and from 100 to 120 kDa indicates the presence of LMW and HMW components which could be attributed to albumins-globulins and glutenin polypeptide chains, respectively, in accordance to previous studies that have

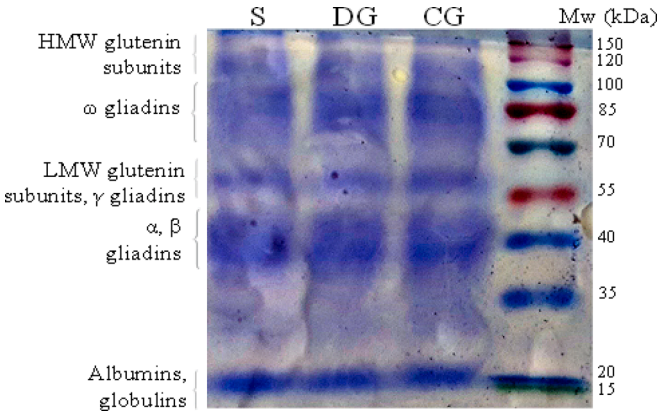

Fig. 1. SDS-PAGE of G proteins. S: G extract in ethanol–water 70% (v/v) from durum wheat semolina, DG: G extract in ethanol–water 70% (v/v) from gluten recovered from durum wheat semolina; CG: G extract in ethanol–water 70% (v/v) from commercial gluten from wheat.

observed by SDS-PAGE the slight presence of albumins-globulins (Dahesh et al., 2014), and glutenin subunits (MW of 94–111 kDa) (Žilić et al., 2011) upon extraction with 70% aqueous ethanol.

By SDS-page analysis, it was proved that the G extracts from different sources (S, DG, and CG) by a 70% hydroalcoholic solution were comparable to each other, supporting the use of a single-step extraction process of G from durum wheat semolina, because of its equivalent efficacy to more complex processes.

3.2. *Effect of Gliadin/Grape pomace extract (G/GP) ratio on particle fabrication*

The dH, PdI, and ζ-potential of the colloidal particles were measured at different G/GP ratios, as shown in Fig. 2a and b. G particles presented a nanometric size, with a dH of 160.3 ± 2.5 nm at pH of 5.1, which, despite the differences in G sources, system composition, and preparation methods, is in good agreement with the values from 200 to 260 nm, reported in previous studies (Wu et al., 2018; Joye et al., 2015). G-based nanoparticles encapsulating GP showed a stable dH ranging from 92.9 ± 4.1 nm to 102.7 ± 2.9 nm, while non -encapsulated GP exhibited a dH value of 940 ± 53.2 nm.

The addition of polyphenols was found to affect the physical characteristics of the colloidal systems, especially a reduction in particle size, which is attributable to the conjugation interactions between proteins and polyphenols.

Several authors have previously observed that colloidal particles formulated with protein isolates exhibited a significant decrease in mean particle size when loaded with polyphenols (Hansen et al., 2021). Similar trends were observed by Xue et al. (2020), who investigated the fabrication of colloidal systems based on soy protein isolate for the encapsulation of cyanidin-3-galactoside. The saturation of binding sites on proteins with polyphenols might induce the disruption of protein–protein hydrogen bonds, increasing repulsive interactions, hence preventing the formation of larger aggregates (Hansen et al., 2021).

In this work, the protein-polyphenols interactions were also confirmed by a bathochromic effect, shown in Fig. 2.d, attributable to the G molecules covering the GP components.

Generally, the addition of polyphenols modifies the protein network and microenvironments, affecting the polydispersity and stability of the system (Li et al., 2021). The obtained colloidal systems displayed a low polydispersity index (PdI) indicating narrow size distribution, ranging from 0.16 ± 0.01 to 0.27 ± 0.01. In contrast, GP precipitated in a polydisperse form, revealed by a very high PdI value of 0.56 ± 0.06. The use of G as a carrier material enabled to obtain homogeneously distributed and monodispersed colloidal particles in the nanometric range, as can be deduced also by the visual appearance of the systems after precipitation (Fig. 2.c). This is in accordance with Wang et al. (2021), who proved that G formed a more stable and ordered structure upon the addition of quercetin, due to the high-affinity interactions between G and quercetin.

The colloidal systems were also characterized through the determination of ζ-potential. G particles at a pH of 5.64 presented a zeta-potential of 11.5 ± 0.8 mV, coherently with the value of 13 mV reported by Joye et al. (2015).

The highest ζ-potential value (21.8 ± 0.6 mV) was observed for the colloidal system with the highest GP loading (G/GP = 10:10), while the system formulated without the addition of G (GP) exhibited the lowest detected ζ-potential value (10.0 ± 3.8 mV). Generally, the higher the

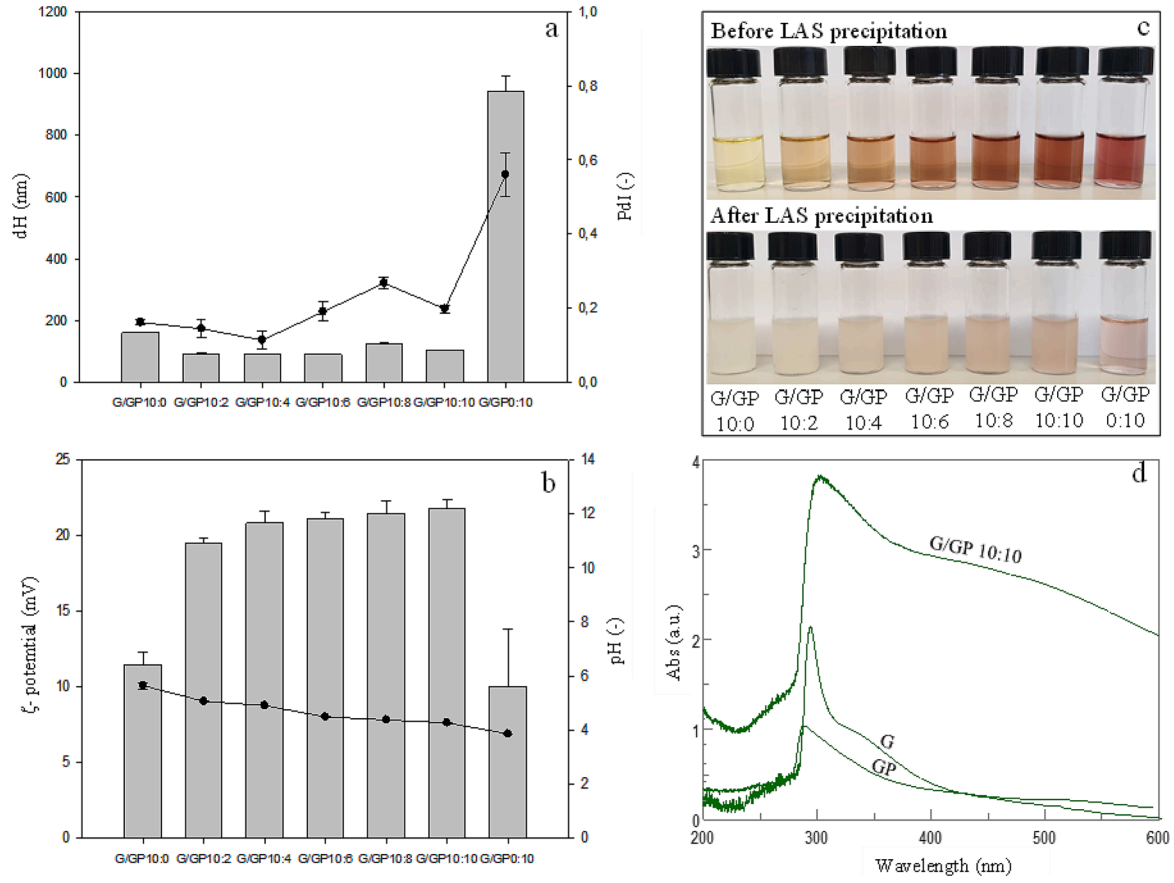

Fig. 2. Effect of formulation on morphological and physicochemical properties of G/GP colloidal particles. Hydrodynamic diameter dH and polydispersity index PdI (a), ζ-potential and pH (b) of the colloidal suspensions at different G/GP mass ratios, photographs of the G/GP suspensions at different mass ratios are shown before (above) and after (below) LAS precipitation (c), amd UV–Vis spectra of GP, G, G-GP 10:10 colloidal particles (d). The bar chart and the scatter chart in (a) refer to dH and PdI, the bar chart and the line chart in (b) refer to ζ-potential and pH, respectively.

magnitude of ζ-potential, the more intense the repulsive forces, eventually becoming strong enough to overcome the Van Der Waals attractive forces, therefore increasing the stability of the colloidal particles (Selvamani, 2019).

Remarkably, all the natural pH values of the obtained colloidal systems were far from the G isoelectric point (6.5), where a modification of the tertiary G structure can occur, reducing the probability to form larger aggregates.

3.3. Effect of Gliadin/Gum arabic ratio on particle formulation

To investigate the effect of GA as a stabilizer of the (blank) colloidal particles, the dH, PdI, and ζ-potential were measured at different G/GA ratios, as shown in Fig. 3a and b. As already mentioned, with a pH of 5.1, G particles presented a dH value in the nanometric range of 160.3 ± 2.5 nm, and a monodisperse PdI value of 0.24 ± 0.01. The precipitation of G in a GA aqueous solution resulted in the formation of complex colloidal particles of larger size than during precipitation in water alone. The highest dH value of 2760 ± 185 nm was observed at low GA concentrations (G:GA ratio = 10:1 w/w), likely because of bridging flocculation: GA molecules, at excessively low concentrations to fully cover the particle surface, form bridges among the G particles, inducing aggregation and precipitation. This observation is in accordance with previous findings demonstrating that at low polysaccharide concentrations, bridging flocculation occurred for different complex particles, such as G stabilized with GA (Wu et al., 2018), casein micelles stabilized with pectin (Goh et al., 2019) and zein stabilized with GA (Gali et al., 2022). Generally, this phenomenon occurs due to an insufficient concentration of negatively-charged polysaccharides to completely cover the newly created positively charged protein surface (Fig. 3c).

As the GA concentration increased (G/GA ratio ≤ 2:1), it was able to fully cover the G particle surface, improving particle stability by electrostatic repulsive interactions and steric stabilization (Fig. 3c). Stable colloidal particles were obtained with a dH value around 500 nm and a PdI < 0.13. In particular, the lowest dH and PdI values were obtained at a G/GA ratio of 1:1 (506.6 ± 5.0 nm and 0.12 ± 0.01, respectively).

The further addition of GA beyond the saturation concentration led to a significant increase in the particle size up to about 1800 nm, and the consequent phase separation and formation of a dense polymer network because of depletion interactions (Goh et al., 2019). Interestingly, the same trend was observed by Jiang et al. (2020) for G particles, whose size, over the addition of citrus pectin, tended to increase significantly due to the multilayer deposition phenomenon (Jiang et al., 2020).

With a pH of 5.1, G particles exhibited a positive net charge, with a ζ-potential of + 11.2 ± 0.9 mV; conversely, GA suspensions showed a negative charge, with a ζ-potential of −15.4 ± 0.8 mV. These values are

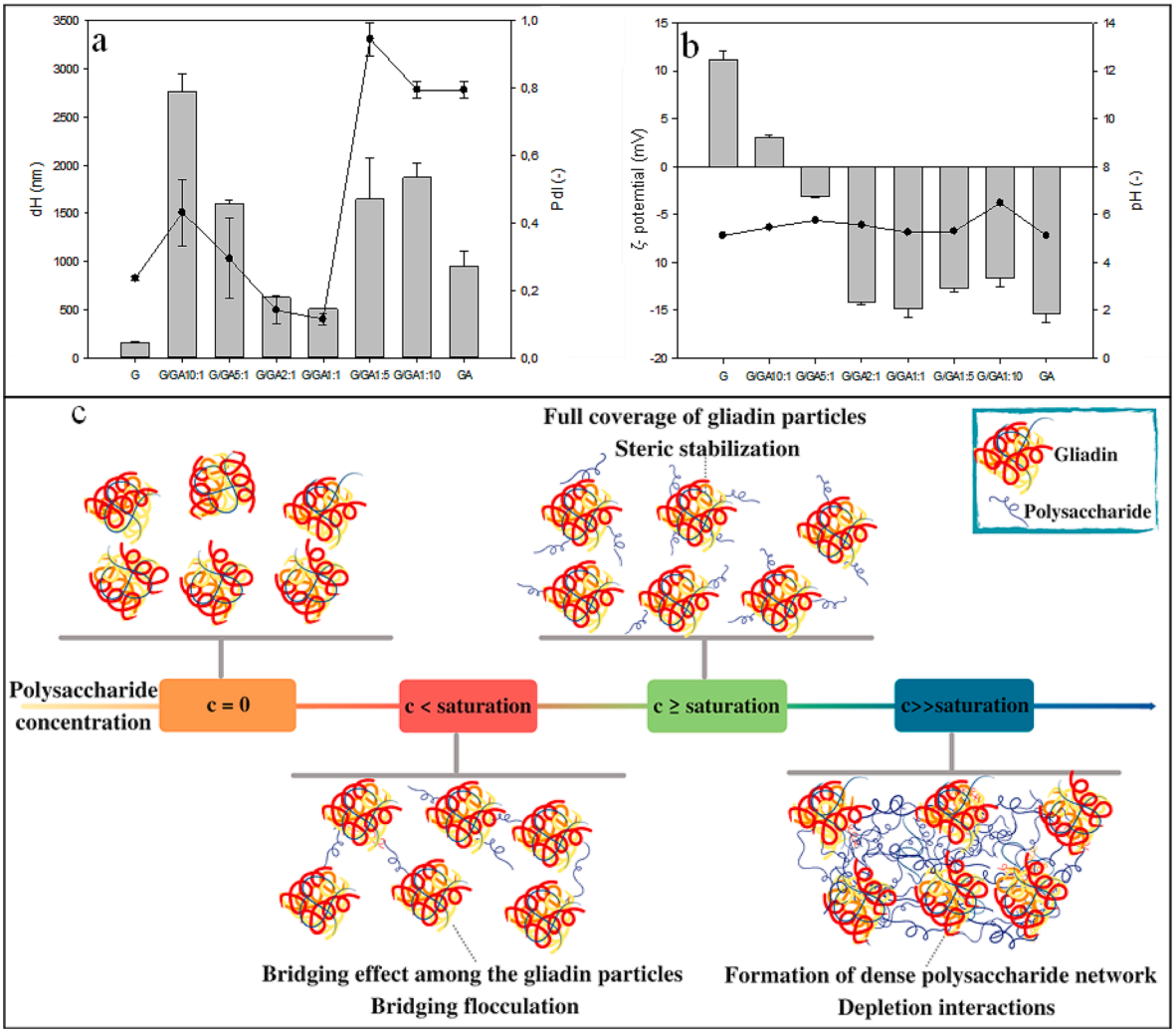

Fig. 3. Effect of formulation on the size distribution and surface charge of G/GA particles. Hydrodynamic diameter dH, and polydispersity index PdI (a), ζ-potential, and pH (b) of the colloidal suspensions at different G/GA mass ratios, schematic representation of the interaction mechanism between G nanoparticles and GA polysaccharides is also depicted (c). The bar plot and the scatter plot in (a) refer to dH and PdI, the bar plot and the line plot in (b) refer to ζ-potential and pH, respectively.

in good agreement with the values reported by Wu et al. (2018) for G particles (~13 mV), and GA solution (~-25 mV) at pH 5.

The ζ-potential values of G/GA particles are affected by the surface saturation by GA. At a G/GA ratio of 10:1, the GA concentration was insufficient to cause the switch of the surface charge (a ζ-potential of + 3.05 ± 0.3 mV was observed), while at higher GA concentrations (G/GA ratios ≤ 5:1) the inversion of ζ-potential from positive to negative values occurred, tending towards the ζ-potential of pure GA as GA concentration increased. As already discussed, this behavior, in agreement with previous results (Wu et al., 2018), confirmed that the full coverage of the surface of G particles by anionic GA polymers was achieved.

3.4. Effect of different extraction procedures on extracts' bioactivity

Flavonoids are the largest group of naturally occurring phenolic compounds in the grape pomace, with epicatechin representing the most abundant flavonoid contained in this agri-food by-product. They possess strong antioxidant and anti-inflammatory properties (Carpentieri et al., 2022a).

The HPLC-PDA analysis of the obtained hydroalcoholic extracts (G/GP 0:10, G/GP10:10, S + GP, GP + S, and co-extract) shows that, regardless of the adopted extraction procedure, the main phenolic compounds in the GP extract corresponds to epicatechin (peak 2), followed by rutin (peak 5), naringin (peak 4), p-coumaric acid (peak 3), and chlorogenic acid (peak 1), detected at elution times of 16.48, 21.50, 21.21, 18.51, and 16.03 min, respectively (Fig. 4a and b).

In addition to the identified phenolic compounds, other unidentified compounds were also detected. Two peaks were recorded at 22.20, and 23.71 min: considering the influence on the phenolic profile of different factors, such as cultivar, variety, growing location, climate, ripeness degree, vinification systems, extraction protocols, and apparatus, they can be attributed to myricetin and fertaric acid, respectively (Ramirez-

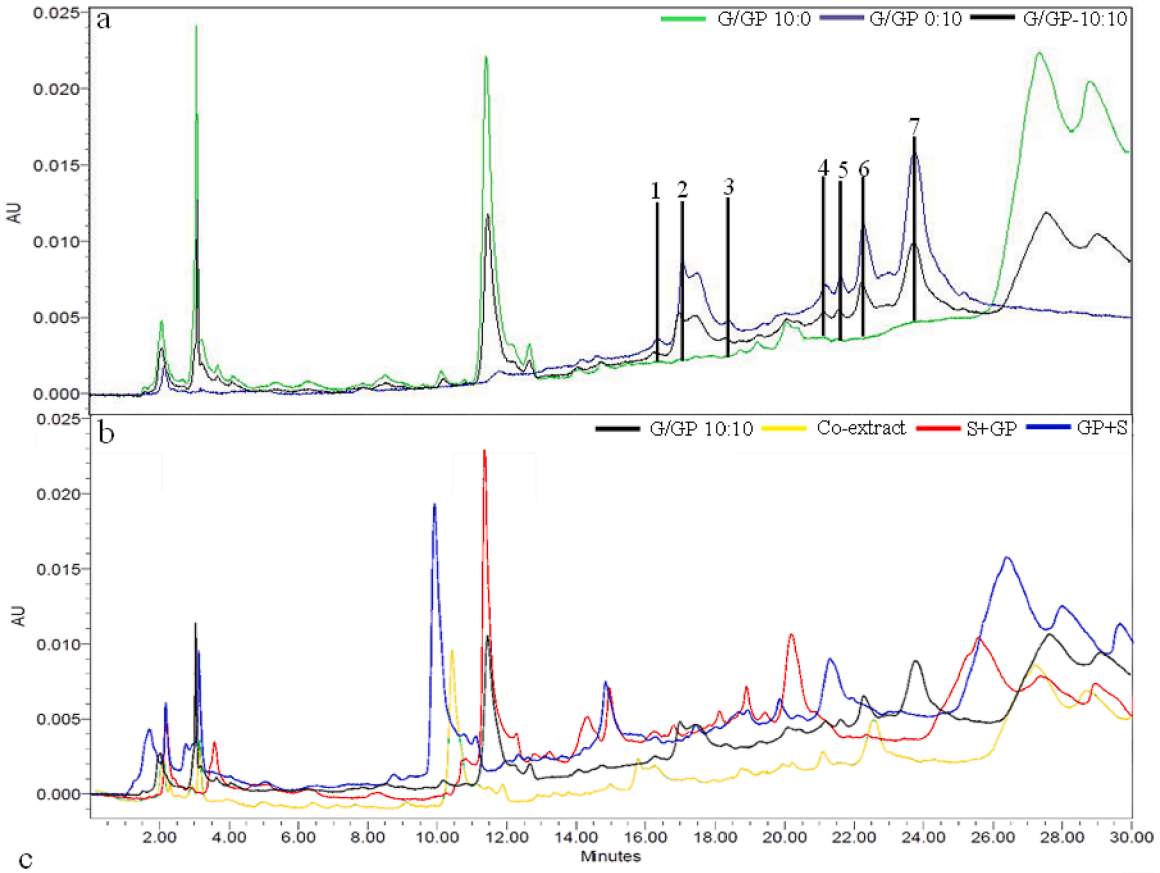

c

Peak	Compound	Concentration (mg/g_{DW})					
		G/GP 10:0	G/GP 0:10	G/GP 10:10	Co-extract	S+GP	GP+S
1	Chlorogenic acid	0.008	0.06	0.06	0.06	0.06	0.06
2	Epicatechin	nd	0.60	0.52	0.32	1.12	1.18
3	p-coumaric acid	0.006	0.10	0.08	0.08	0.08	0.08
4	Naringin	nd	0.06	0.08	0.10	0.22	0.12
5	Rutin	nd	0.10	0.10	0.18	0.40	0.28

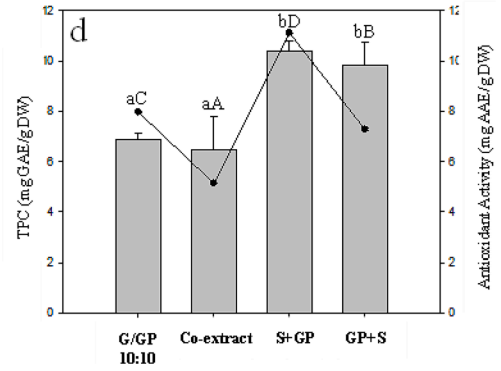

Fig. 4. HPLC/PDA chromatograms of G-based particles loaded with different extracts. Chromatograms of G/GP10:0, G/GP0:10, and G/GP10:10 (a), G/GP10:10, co-extract, S + GP, and GP + S (b), concentrations (mg/gDW) of the identified phenolic compounds (c), and the Total Phenolic Content (TPC) of the investigated extracts (d). Peak identification: chlorogenic acid (1); epicatechin (2); p-coumaric acid (3); naringin (4), rutin (5); unidentified compound (6); unidentified compound (7). Bars bearing different letters (lowercase for TPC, uppercase for the antioxidant activity) indicate significant difference ($p < 0.05$).

Lopez et al., 2014). Likewise, in the extract from semolina (G/GP10:0) another unidentified wide peak at an elution time of 11.30 min was detected. Literature data suggest that this peak could correspond to hydroxybenzoic acid, which is the second most abundant free phenolic acid (27%) in wheat semolina after ferulic acid (37%) (Bueno-Herrera & Pérez-Magariño, 2020).

Interestingly, all the above-mentioned phenolic compounds found both in the extract from semolina (G/GP10:0) and in the extract from GP (G/GP0:10), were detected, as expected, both in the G/GP 10:10 system, given by the combination of the two hydroalcoholic extracts and in the other systems (co-extract, S + GP, GP + S) obtained from different combinations of the extraction procedures.

The HPLC-PDA analysis of the hydroalcoholic extract, showed that the epicatechin content belonging to GP ranged from 0.32 mg/g_{DW} to 1.18 mg/g_{DW} (Fig. 4c). These values are consistent with the data previously reported by other authors, who found that catechins were the most abundant non-anthocyanin compounds in red grape pomace extracts, with the epicatechin possessing the highest concentration (0.25–1.95 mg/g_{DW}) (Caldas et al., 2018; Negro et al., 2021).

Moreover, regardless of the applied extraction procedure, the phenolic profiles of the investigated extracts, such as G/GP10:10, co-extract, S + GP, and GP + S (Fig. 4b), appeared similar and consistent with each other. However, the different concentrations of the identified peaks (Fig. 4c) demonstrated that the different extraction methods utilized greatly affected the extraction yield of the phenolic compounds.

More specifically, extracting sequentially first G from semolina and then phenolic compounds from GP led to the highest amount of phenolics in the extract (S + GP), enhancing the recovery of the identified compounds by almost 1.24 times compared to mixing of the two separately obtained hydroalcoholic extracts G/GP10:10. Conversely, the concurrent extraction (co-extract) did not significantly change the extractability of phenolics from GP compared to the two-step separated extraction G/GP10:10. These findings can be likely attributed to the loss of some phenolic compounds because of their adsorption in semolina particles. Similarly, also the adsorption of the solvent in wheat semolina might have lowered solvent availability, reducing phenolics extractability.

In good agreement with the chromatographic profiles, Total Phenolic Content (TPC) values reported in Fig. 4d, show how the TPC of S + GP almost doubled compared to the separate extract of G/GP10:10 and the co-extract, as also corroborated by the greater color intensification of S + GP compared with the other extracts investigated (Figure S3).

These observations can be explained by the high affinity of the wheat proteins, mainly G, for polyphenols, with which they form soluble or insoluble protein–polyphenol complexes (van Buiten & Elias, 2021), increasing solvent affinity for polyphenols and, hence, enabling a better extraction of the intracellular phenolic compounds from GP. These results support the use of this extraction procedure (S + GP) as an effective strategy to improve the extraction process in terms of recovery yield of the target intracellular bioactive compounds.

3.5. Encapsulation efficiency (EE) of GP extracts

The encapsulation efficiencies of the obtained systems without the addition of GA (G/GP 10:10, co-extract, S + GP, GP + S) and with the addition of GA (G/GP/GA 10:10, co-extract/GA, S + GP/GA, GP + S/GA) in terms of TPC determined by the Folin-Ciocalteu method (EE_{TPC}), and of antioxidant activity determined by the FRAP assay (EE_{AA}) are reported in Table 1.

Results showed that the highest EE was obtained for S + GP/GA particles, with a value of 43.8 ± 0.8% for EE_{TPC}, and 52.6 ± 4.5% for EE_{AA}, while values of 40.2 ± 1.8% and 30.4 ± 3.5%, respectively, were obtained for S + GP without the addition of GA. The higher EE detected upon the addition of GA, especially in terms of antioxidant activity, indicates that GA contributed to significantly improving the encapsulation efficiency of GP-rich extracts.

The same trend was observed also for G/GP, and GP + S samples. In the case of the co-extract, no significant statistical differences in EE_{TPC} and EE_{AA} were detected between co-extract and co-extract/GA. Although not statistically significant, the slight decrease in the EE values upon the addition of GA could be attributed to the adsorption of GP phenolic molecules by the semolina solid residue during the co-extraction process, promoting both a lower extraction yield in terms of TPC and their possible encapsulation by the semolina proteins. Thus, although these considerations should be confirmed by more in-depth studies, the addition of GA may not significantly further contribute to an increase in encapsulation efficiency.

The enhancement of the encapsulation efficiency in complex G particles was previously detected for curcumin-loaded G nanoparticles upon the addition of tremella polysaccharide, which further increased the already high initial EE value. This behavior could be attributed to the polysaccharide forming a thick layer around the nanoparticles, which increased the electrostatic repulsion between the nanoparticles and hindered the release of curcumin (Zhang et al., 2022). Similarly, the addition of GA to resveratrol-loaded G nanoparticles (W. Wu et al., 2020), and the addition of rhamnolipid to curcumin-loaded G nanoparticles (Chen et al., 2021) significantly increased the encapsulation efficiency in the complex nanoparticles.

Remarkably, regardless of the formulation of the colloidal systems, and consistently with previous findings (Gali et al., 2022; Zhang et al., 2022), the addition of GA significantly increased the particle size of the colloidal particles. For example, as a result of the addition of GA as a stabilizer, the dH of zein colloidal particles loaded with a rutin-rich extract underwent a slight but significant increase (Gali et al., 2022). Likewise, after adding tremella polysaccharide to curcumin/G nanoparticles, the mean particle size of nanoparticles increased due to the aggregation (Zhang et al., 2022).

The PdI values for both G and G/GA particles showed that the different investigated formulations did not alter the monomodal distribution (PdI < 0.3) of the colloidal suspensions. In addition, the ζ-potential of the different colloidal suspensions exhibited a non-statistically

Table 1
Hydrodynamic diameter (dH), polydispersity (PdI), ζ-potential, and encapsulation efficiency of the different GP-loaded colloidal particles. Encapsulation efficiency (EE) was assessed by the Folin-Ciocalteu method for total polyphenols, by FRAP method for antioxidant activity, and by HPLC for epicatechin and unidentified compounds "Peak 6" and "Peak 7".

Formulation	dH (nm)	PdI (-)	ζ-potential (mV)	EE_{TPC} (%)	EE_{AA} (%)	EE_{HPLC} (%)		
						Epicatechin (Peak 2)	Peak 6	Peak 7
G/GP	102.2 ± 2.9^{a}	0.20 ± 0.01^{abc}	21.5 ± 0.6^{b}	24 ± 3.1^{a}	25 ± 2.2^{ab}	25.2 ± 1.2^{a}	25.1 ± 1.2^{c}	5.4 ± 0.7^{b}
G/GP/GA	338 ± 7.9^{d}	0.18 ± 0.08^{abc}	−20.1 ± 0.9^{a}	43.6 ± 2.3^{b}	38.6 ± 1.7^{c}	31.2 ± 1.1^{abc}	34 ± 1.4	22 ± 1.4 ^{cd}
Co-extract	166.4 ± 7.9^{b}	0.16 ± 0.05^{ab}	20.01 ± 0.5^{b}	29.9 ± 0.8^{a}	23.9 ± 2.1^{ab}	34.5 ± 2.1^{bc}	15.5 ± 1.7^{c}	18.7 ± 1.5^{a}
Co-extract/GA	238.9 ± 4.0^{c}	0.15 ± 0.02^{ab}	−24.2 ± 0.7^{a}	27.8 ± 2.5^{a}	17.6 ± 2.2^{a}	29.3 ± 1.6^{ab}	23.9 ± 2.7^{c}	22.2 ± 1.3^{ab}
S + GP	181.5 ± 2.6^{b}	0.28 ± 0.01^{d}	21.02 ± 0.5^{b}	40.2 ± 1.8^{b}	30.4 ± 3.5^{bc}	44.2 ± 1.7^{d}	42.4 ± 2.9^{c}	37.9 ± 2.8^{d}
S + GP/GA	331.9 ± 0.8^{d}	0.09 ± 0.01^{a}	–23.7 ± 0.7^{a}	43.8 ± 0.8^{b}	52.6 ± 4.5^{d}	63.5 ± 3.7^{f}	62.9 ± 3.2^{c}	45.6 ± 2.5^{f}
GP + S	253.7 ± 2.9^{c}	0.27 ± 0.01 ^{cd}	21.2 ± 0.5^{b}	22.1 ± 3.3^{a}	26.9 ± 3.1^{ab}	36.8 ± 2.5 ^{cd}	28.5 ± 1.5^{c}	39.8 ± 1.6^{bc}
GP + S/GA	375.9 ± 20.1^{e}	0.23 ± 0.03^{bcd}	–23.1 ± 0.7^{a}	27.7 ± 2.1^{a}	32.2 ± 4.4^{bc}	53.3 ± 2.5^{e}	52.1 ± 3.3^{c}	40.6 ± 2.3^{e}

Results are means ± SD of three measurements. Values in each column with different superscript letters are significantly different ($p < 0.05$).

significant variation upon the different extraction procedures. In the case of the colloidal systems without GA, the ζ-potential slightly decreased from + 21.5 ± 0.1 to + 20.1 ± 0.5 mV, whereas, for the systems with the addition of GA, the ζ-potential varied from − 20.1 ± 0.9 to − 24.2 ± 0.7 mV.

The EE of the three most abundant phenolic compounds (EE_{HPLC}) detected in G nanoparticles (epicatechin, peak 6, and peak 7 (Fig. 4)), with and without the addition of GA are also reported in Table 1. Similarly to the EE evaluated by Folin Ciocalteu and FRAP assay, the addition of GA induced the enhancement of EE_{HPLC}, which was 63.5 ± 6.7% for S + GP/GA, and 31.2 ± 1.1% for S + GP, highlighting the key role of molecular interactions of the extract components and G with GA. Indeed, a previous study reported the use of G/GA nanoparticles to efficiently encapsulate resveratrol (Wu et al., 2020).

It is interesting to note that S + GP without GA exhibited a high value of EE_{HPLC} for epicatechin (44.2 ± 1.7%), even higher than the EE_{HPLC} detected for G/GP/GA (31.2 ± 1.1%) obtained by the combination of the two separately-obtained extracts (GP from grape pomace and G from semolina) with the addition of GA. This observation further supports the hypothesis that strong non-covalent molecular interactions occur between G already present in the extracting solvent, previously obtained from the semolina hydroalcoholic extraction, and the phenolic compounds recovered from grape pomace.

These findings, consistent with the previously discussed results (Section 3.4), show that the investigated extraction methods greatly affected not only the extraction yield but also the encapsulation efficiency of the obtained systems. More specifically, the reported considerations suggest that especially the extraction method related to S + GP could represent a promising processing approach for the achievement of natural-based G/GP nanoparticles, fabricated through a simple and versatile extraction process.

Therefore, after these comprehensive considerations and to further support the findings achieved so far, S + GP, G/GP, and GP + S were selected, as the most promising systems, for follow-up in vitro digestion studies.

3.6. *In vitro digestion*

The effect of simulated digestion on G-based colloidal particles G/GP, S + GP, GP + S, and on the same systems with GA addition, G/GP/GA, S + GP/GA, GP + S/GA, was investigated by monitoring the release of TPC during oral, gastric and intestinal digestion phases using in vitro digestive models, with the results shown in Fig. 5a-5b-5c. Additionally, the release of epicatechin, measured through HPLC-PDA analysis, from S + GP and S + GP/GA systems, which showed the highest EE_{HPLC}, as previously discussed, is reported in Fig. 5d.

Results in Fig. 5a demonstrate that the bioaccessibility of TPC from free GP-rich extract (G/GP 0:10) was significantly ($p < 0.05$) lower than for G/GP 10:10 and G/GP/GA. Similar results were obtained by He et al. (2022), who found that the bioaccessibility of phloretin increased significantly after its encapsulation in G/sodium carboxymethyl cellulose nanoparticles compared to the bioaccessibility of free phloretin.

Overall, about 40% of the TPC was released from the obtained colloidal particles at pH 3.0 in simulated gastric fluid (SGF) after 60 min of digestion. Nonetheless, a slight low release and a sharp increase in TPC were detected for all the investigated systems after 120 min of

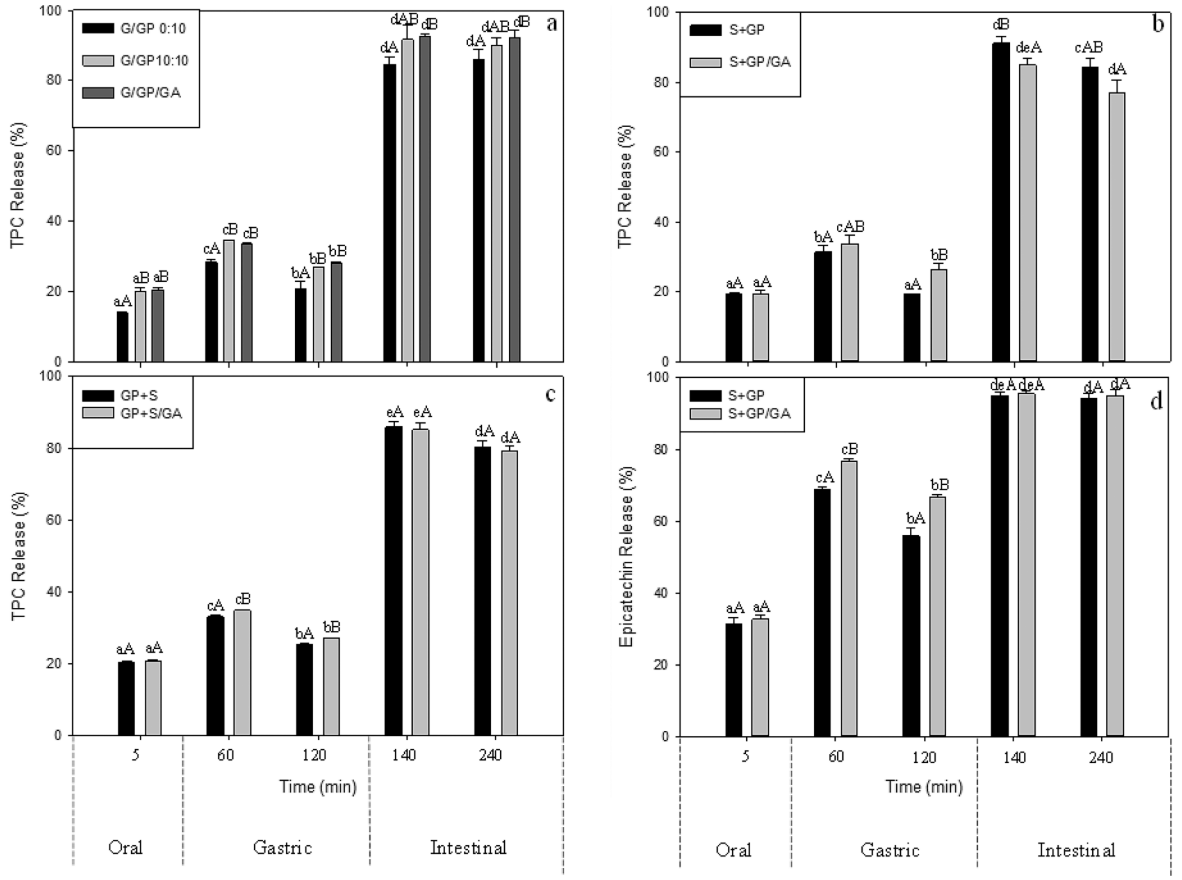

Fig. 5. Effect of simulated digestion on the release of BACs from the colloidal particles. Release of Total Phenolic Content (TPC) from G/GP0:10, G/GP10:10, and G/GP/GA particles (a), S + GP, S + GP/GA particles (b), GP + S, GP + S/GA particles (c), and of epicatechin from S + GP and S + GP/GA particles(d). Results are means ± SD of three measurements. Bars related to the same sample at different digestion times bearing different lowercase letters, and bars related to different samples at the same digestion time bearing different uppercase letters indicate significant differences ($p < 0.05$).

simulated gastric digestion, and after the first 20 min of intestinal digestion, respectively (Fig. 5a, 5b, 5c). Previous studies indicated that the acid-base change of the medium that undergo the digestate after the gastric phase can promote the release of phenolic substances, which was due to the deprotonation of the hydroxyl group in the aromatic ring, which helps to improve the antioxidant activity of phenolic compounds (Luo et al., 2022). The intestinal phase causes a much higher increase in TPC indicating that the action of pancreatin and pH at this stage effectively induces the release of polyphenols, promoting the marked degradation of macromolecules in sugars and small peptides/amino acids (Luo et al., 2022). Indeed, Li et al. (2022) showed that the studied micelles presented a pH-dependent release, with a low phenolic release in simulated gastric fluid, and a sustained release in simulated intestinal fluid.

Remarkably, the addition of GA significantly increased the release of TPC for all the different formulations investigated during the simulated gastric digestion, with no statistically significant differences in the simulated intestinal digestion except for S + GP where a slight but significant decrease was observed during the first 20 min. GA addition indirectly implies controlled-release properties during digestion, even if, the dynamic condition of digestion, such as changing the pH, ionic strength, dilution, enzyme activity, also adds complexity and can affect possible TPC degradation or interactions between macromolecules, including GA, and phenolic compounds recovered during the extraction process, hindering their release. These aspects need to be better addressed by future studies on the topic.

Zeng et al. (2019) assessed that over 35% of loaded curcumin was released from G-chitosan nanoparticles during SGF pepsin digestion.

Interestingly, Fig. 5d demonstrates that 76.8% of epicatechin was released from S + GP/GA particles already after 60 min of digestion in SGF, and epicatechin was almost completely released after the first 20 min of digestion in simulated intestinal fluid (SIF) (95.6%), with a non-significant increase in the release during the remaining 120 min of simulated intestinal digestion. This behavior can be attributed to the quick dissolution of GA during the gastric phase of the simulated digestion (Gali et al., 2022).

Conversely, the release of epicatechin from S + GP particles during the gastric phase reached 68.8% after 60 min in SGF. Previous studies have reported similar observations for rutin-loaded zein nanoparticles (Gali et al., 2022), where a higher release of the encapsulated compound in SGF was observed when rutin was loaded in GA-coated zein particles (98.8%) than when loaded in plain zein particles (81.3%).

Recent findings suggest that this behavior can be attributed to the good mucoadhesive properties of G particles during gastrointestinal digestion, especially because of its hydrolysis by pancreatin during the intestinal phase, hence promoting the bioaccessibility of the encapsulated compounds (Gali et al., 2022, Zhang et al., 2022; He et al., 2022). Nonetheless, the differences in the trend of epicatechin release compared with that of TPC from S + GP and S + GP/GA (Fig. 5b and 5d), could be attributed to the fact that the TPC, including all the polyphenols present in the analyzed extracts and characterized by different resistances to the gastrointestinal conditions, result from the balance of phenolics that have been released, degraded, or converted into new compounds. It should be also noted that the Folin Ciocalteu assay is not specific for polyphenols, since other reducing agents may react with the reagent. In addition, the pH susceptibility of structurally different plant phenolic compounds, stored in cell vacuoles and walls, depends heavily on the phenol structure. The structural characteristics of epicatechin, characterized by two separate aromatic systems, due to the spatial arrangement between an OH group and the π-electron system governing the extent of π-orbital overlap, affect the susceptibility to chemical changes, making epicatechin more resistant to pH-induced degradation (Friedman & Jürgens, 2000).

The obtained results indicated that both G and G/GA nanoparticles could be potentially applied as suitable natural-based delivery systems for valuable phenolic compounds from grape pomace able to control their bioaccessibility during gastrointestinal digestion. Moreover, the extraction procedure, affecting the nature of the molecular interactions between G and the extracted polyphenols, might be exploited also to affect encapsulation efficiency and release during digestion. However, this aspect, which is particularly promising in the development of facile and versatile encapsulation methods with natural ingredients, needs to be better investigated in future studies.

4. Conclusions

All-natural, gliadin(G)-based colloidal delivery systems were developed for the encapsulation of grape pomace (GP) extracts, rich in bioactive compounds, showing a positive contribution to preserving their bioactivity and improving their bioaccessibility.

The addition of gum arabic (GA) as a stabilizing agent significantly increased the size of the colloidal particles (from dH of 100 nm to 500 nm), because of the interactions of G with GA through hydrogen bonds and electrostatic forces, as well as the encapsulation efficiency of the investigated phenolic compounds.

This work also focused on testing different extraction methods. In particular, the sequential extraction of semolina to recover G, and then using the G-rich hydroalcoholic solution for the subsequent extraction of polyphenols from GP significantly improved the yield of extraction, affecting also the extract composition. The interactions between G and polyphenols, promoted by the sequential extraction process, also enhanced the encapsulating ability of G for the GP phenolic compounds, such as epicatechin.

The most promising obtained colloidal system (S + GP) promoted epicatechin release during simulated digestion, demonstrating to be suitable for the development of an all-natural delivery system for GP polyphenols. These results not only encourage the reintegration of grape processing by-products in the food industry for product functionalization but also suggest that the development of a simple and versatile extraction process could represent an effective strategy to improve extraction yields and promote a better encapsulation of bioactive compounds.

Nonetheless, further studies are required to better elucidate the molecular interactions triggered by the different extraction processes and their role in particle formation and in controlling the release of the payload compounds.

CRediT authorship contribution statement

Serena Carpentieri: Conceptualization, Methodology, Data curation, Investigation, Formal analysis, Writing – original draft, Writing – review & editing. **Giovanna Ferrari:** Supervision, Formal analysis, Funding acquisition, Resources. **Francesco Donsì:** Conceptualization, Methodology, Supervision, Formal analysis, Writing – review & editing.

Declaration of Competing Interest

The authors declare that they have no known competing financial interests or personal relationships that could have appeared to influence the work reported in this paper.

Data availability

Data will be made available on request.

Acknowledgments

The authors would like to thank Eng. Oscar Mauricio Pulgarin Lopez for his help with *in vitro* digestion study and Eng. Sonia Palladino for contributing to the preparation and physicochemical characterization of the nanoparticles.

Appendix A. Supplementary data

Supplementary data to this article can be found online at https://doi.org/10.1016/j.foodchem.2023.136385.

References

Albuquerque, B. R., Heleno, S. A. 8., Oliveira, M. B. P. P., Barros, L., & Ferreira, I. C. F. R. (2021). Phenolic compounds: Current industrial applications, limitations and future challenges. In *Food and Function* (Vol. 12, Issue 1, pp. 14–29). Royal Society of Chemistry. https://doi.org/10.1039/d0fo02324h.

Bueno-Herrera, M., & Pérez-Magariño, S. (2020). Validation of an extraction method for the quantification of soluble free and insoluble bound phenolic compounds in wheat by HPLC-DAD. *Journal of Cereal Science, 93*, Article 102984. https://doi.org/10.1016/J.JCS.2020.102984

Caldas, T. W., Mazza, K. E. L., Teles, A. S. C., Mattos, G. N., Brígida, A. I. S., Conte-Junior, C. A., Borguini, R. G., Godoy, R. L. O., Cabral, L. M. C., & Tonon, R. v. (2018). Phenolic compounds recovery from grape skin using conventional and non-conventional extraction methods. *Industrial Crops and Products*, *111*(May 2017), 86–91. https://doi.org/10.1016/j.indcrop.2017.10.012.

Carpentieri, S., Ferrari, G., & Pataro, G. (2022a). Optimization of pulsed electric fields-assisted extraction of phenolic compounds from white grape pomace using response surface methodology. *Frontiers in Sustainable Food Systems, 6*. https://doi.org/10.3389/fsufs.2022.854968

Carpentieri, S., Larrea-Wachtendorff, D., Donsì, F., & Ferrari, G. (2022b). *Functionalization of pasta through the incorporation of bioactive compounds from agri-food by-products: Fundamentals, opportunities, and drawbacks* (Vol. 122,, 49–65. https://doi.org/10.1016/j.tifs.2022.02.011

Carullo, D., Barbosa-Cánovas, G., & v., & Ferrari, G.. (2021). Changes of structural and techno-functional properties of high hydrostatic pressure (HHP) treated whey protein isolate over refrigerated storage. *LWT, 137*, Article 110436. https://doi.org/10.1016/J.LWT.2020.110436

Chen, S., Ma, Y., Dai, L., Liao, W., Zhang, L., Liu, J., & Gao, Y. (2021). Fabrication, characterization, stability and re-dispersibility of curcumin-loaded gliadin-rhamnolipid composite nanoparticles using pH-driven method. *Food Hydrocolloids, 118*. https://doi.org/10.1016/j.foodhyd.2021.106758

Costa, J. R., Xavier, M., Amado, I. R., Gonçalves, C., Castro, P. M., Tonon, R. V., Cabral, L. M. C., Pastrana, L., & Pintado, M. E. (2021). Polymeric nanoparticles as oral delivery systems for a grape pomace extract towards the improvement of biological activities. *Materials Science and Engineering: C, 119*, Article 111551. https://doi.org/10.1016/J.MSEC.2020.111551

Dahesh, M., Banc, A., Duri, A., Morel, M. H., & Ramos, L. (2014). Polymeric assembly of gluten proteins in an aqueous ethanol solvent. *Journal of Physical Chemistry B, 118* (38), 11065–11076. https://doi.org/10.1021/jp5047134

Friedman, M., & Jürgens, H. S. (2000). Effect of pH on the stability of plant phenolic compounds. *Journal of Agricultural and Food Chemistry, 48*, 2101–2110. https://doi.org/10.1021/jf990489j

Gali, L., Bedjou, F., Ferrari, G., & Donsì, F. (2022). Formulation and characterization of zein/gum arabic nanoparticles for the encapsulation of a rutin-rich extract from Ruta chalepensis L. *Food Chemistry, 367*. https://doi.org/10.1016/j.foodchem.2021.129982

Garcia-Valle, D. E., Bello-Pérez, L. A., Agama-Acevedo, E., & Alvarez-Ramirez, J. (2021). Effects of mixing, sheeting, and cooking on the starch, protein, and water structures of durum wheat semolina and chickpea flour pasta. *Food Chemistry, 360*. https://doi.org/10.1016/j.foodchem.2021.129993

Goh, K. K. T., Teo, A., Sarkar, A., & Singh, H. (2019). Milk protein-polysaccharide interactions. In *Milk Proteins: From Expression to Food* (pp. 499–535). Elsevier. https://doi.org/10.1016/B978-0-12-815251-5.00013-X.

Hansen, M. M., Hartel, R. W., & Roos, Y. H. (2021). Encapsulant-bioactives interactions impact on physico-chemical properties of concentrated dispersions. *Journal of Food Engineering, 302*. https://doi.org/10.1016/j.jfoodeng.2021.110586

He, J. R., Zhu, J. J., Yin, S. W., & Yang, X. Q. (2022). Bioaccessibility and intracellular antioxidant activity of phloretin embodied by gliadin/sodium carboxymethyl cellulose nanoparticles. *Food Hydrocolloids, 122*. https://doi.org/10.1016/j.foodhyd.2021.107076

Horvat, D., Šimić, G., Dvojković, K., Ivić, M., Plavšin, I., & Novoselović, D. (2021). Gluten protein compositional changes in response to nitrogen application rate. *Agronomy, 11*(2). https://doi.org/10.3390/agronomy11020325

Jiang, Y., Zhu, Y., Li, F., Li, D., & Huang, Q. (2020). Gliadin/amidated pectin core–shell nanoparticles for stabilisation of Pickering emulsion. *International Journal of Food Science and Technology, 55*(10), 3278–3288. https://doi.org/10.1111/ijfs.14590

Joye, I. J., Nelis, V. A., & McClements, D. J. (2015). Gliadin-based nanoparticles: fabrication and stability of food-grade colloidal delivery systems. *Food Hydrocolloids, 44*, 86–93. https://doi.org/10.1016/J.FOODHYD.2014.09.008

Lafiandra, D., Sestili, F., Sissons, M., Kiszonas, A., & Morris, C. F. (2022). Increasing the versatility of durum wheat through modifications of protein and starch composition and grain hardness. *Foods, 11*(11), 1532. https://doi.org/10.3390/foods11111532

Li, H., Gao, Z., Xu, J., Sun, W., Wu, J., Zhu, L., … Zhan, X. (2022). Encapsulation of polyphenols in pH-responsive micelles self-assembled from octenyl-succinylated curdlan oligosaccharide and its effect on the gut microbiota. *Colloids and Surfaces B: Biointerfaces, 219*, Article 112857. https://doi.org/10.1016/j.colsurfb.2022.112857

Li, Y., He, D., Li, B., Lund, M. N., Xing, Y., Wang, Y., … Li, L. (2021). Engineering polyphenols with biological functions via polyphenol-protein interactions as additives for functional foods. *Trends in Food Science & Technology, 110*, 470–482. https://doi.org/10.1016/J.TIFS.2021.02.009

Luo, X., Tian, M., Cheng, Y., Ji, C., Hu, S., Liu, H., … Ren, J. (2022). Effects of simulated in vitro gastrointestinal digestion on antioxidant activities and potential bioaccessibility of phenolic compounds from K. coccinea fruits. *Frontiers Nutrition, 9*, 1024651. https://doi.org/10.3389/fnut.2022.1024651

Minekus, M., Alminger, M., Alvito, P., Ballance, S., Bohn, T., Bourlieu, C., … Brodkorb, A. (2014). A standardised static in vitro digestion method suitable for food-an international consensus. *Food and Function, 5*(6), 1113–1124. https://doi.org/10.1039/c3fo60702j

Negro, C., Aprile, A., Luvisi, A., de Bellis, L., & Miceli, A. (2021). Antioxidant activity and polyphenols characterization of four monovarietal grape pomaces from salento (Apulia, italy). *Antioxidants, 10*(9). https://doi.org/10.3390/antiox10091406

Padalino, L., Mastromatteo, M., Lecce, L., Spinelli, S., Conte, A., & del Nobile, M. A. (2015). Effect of raw material on cooking quality and nutritional composition of durum wheat spaghetti. *International Journal of Food Sciences and Nutrition, 66*(3), 266–274. https://doi.org/10.3109/09637486.2014.1000838

Ramirez-Lopez, L. M., McGlynn, W., Goad, C. L., & Mireles DeWitt, C. A. (2014). Simultaneous determination of phenolic compounds in Cynthiana grape (Vitis aestivalis) by high performance liquid chromatography-electrospray ionisation-mass spectrometry. *Food Chemistry, 149*, 15–24. https://doi.org/10.1016/j.foodchem.2013.10.078

Rani, M., Siddiqi, R. A., Sogi, D. S., & Gill, B. S. (2022). Comparative evaluation of amino acid composition and protein profile of gliadin from different extraction protocols. *Cereal Chemistry, 99*(1), 194–206. https://doi.org/10.1002/cche.10491

Schalk, K., Lexhaller, B., Koehler, P., & Scherf, K. A. (2017). Isolation and characterization of gluten protein types from wheat, rye, barley and oats for use as reference materials. *PLoS ONE, 12*(2). https://doi.org/10.1371/journal.pone.0172819

Selvamani, V. (2019). Stability Studies on Nanomaterials Used in Drugs. *Characterization and Biology of Nanomaterials for Drug Delivery: Nanoscience and Nanotechnology in Drug Delivery, 425–444*. https://doi.org/10.1016/B978-0-12-814031-4.00015-5

Shewry, P. (2019). *What is gluten—Why is it special? In Frontiers in Nutrition* (Vol. 6). https://doi.org/10.3389/fnut.2019.00101

Su, C. R., Huang, Y. Y., Chen, Q. H., Li, M. F., Wang, H., Li, G. Y., & Yuan, Y. (2021). A novel complex coacervate formed by gliadin and sodium alginate: Relationship to encapsulation and controlled release properties. *LWT, 139*. https://doi.org/10.1016/j.lwt.2020.110591

Tateo, F., (1980). Sfarinati di frumento. In Chiriotti Editori, *Analisi dei prodotti alimentari* (pp. 219-2020). ISBN 978-88-85022-10-2.

van Buiten, C. B., & Elias, R. J. (2021). Molecular sciences gliadin sequestration as a novel therapy for celiac disease: a prospective application for polyphenols. *Polyphenols. Int. J. Mol. Sci, 22*. https://doi.org/10.3390/ijms22020595

Wang, Q., Tang, Y., Yang, Y., Lei, L., Zhao, J., Zhang, Y., … Ming, J. (2021). Combined effects of quercetin and sodium chloride concentrations on wheat gliadin structure and physicochemical properties. *Journal of the Science of Food and Agriculture, 101* (6), 2511–2518. https://doi.org/10.1002/jsfa.10877

Williams, P.A. & Phillips, G.O. (2021) Exudate gums, Gum Arabic. In P.A. Williams, & G. O. Phillips (Eds.), *Handbook of Hydrocolloids (Third Edition)* (pp. 627-652). ISBN: 9780128242216.

Wu, W., Kong, X., Zhang, C., Hua, Y., & Chen, Y. (2018). Improving the stability of wheat gliadin nanoparticles – effect of gum arabic addition. *Food Hydrocolloids, 80*, 78–87. https://doi.org/10.1016/j.foodhyd.2018.01.042

Wu, W., Kong, X., Zhang, C., Hua, Y., Chen, Y., & Li, X. (2020). Fabrication and characterization of resveratrol-loaded gliadin nanoparticles stabilized by gum Arabic and chitosan hydrochloride. *LWT, 129*. https://doi.org/10.1016/j.lwt.2020.109532

Wu, X., Hu, Q., Liang, X., & Fang, S. (2022). Fabrication of colloidal stable gliadin-casein nanoparticles for the encapsulation of natamycin: Molecular interactions and antifungal application on cherry tomato. *Food Chemistry, 391*. https://doi.org/10.1016/j.foodchem.2022.133288

Xue, F., Li, C., & Adhikari, B. (2020). Physicochemical properties of soy protein isolates-cyanidin-3-galactoside conjugates produced using free radicals induced by ultrasound. *Ultrasonics Sonochemistry, 64*, Article 104990. https://doi.org/10.1016/J.ULTSONCH.2020.104990

Yang, S., Liu, L., Chen, H., Wei, Y., Dai, L., Liu, J., … Gao, Y. (2021). Impact of different crosslinking agents on functional properties of curcumin-loaded gliadin-chitosan composite nanoparticles. *Food Hydrocolloids, 112*, Article 106258. https://doi.org/10.1016/J.FOODHYD.2020.106258

Zeng, Q. Z., Li, M. F., Li, Z. Z., Zhang, J. L., Wang, Q., Feng, S. L., Su, D. X., He, S., & Yuan, Y. (2019). Formation of gliadin-chitosan soluble complexes and coacervates through pH-induced: relationship to encapsulation and controlled release properties. *LWT, 105*, 79–86. https://doi.org/10.1016/j.lwt.2019.01.071

Zhang, X., Wei, Z., Wang, X., Wang, Y., Tang, Q., Huang, Q., & Xue, C. (2022). Fabrication and characterization of core-shell gliadin/tremella polysaccharide nanoparticles for curcumin delivery: Encapsulation efficiency, physicochemical stability and bioaccessibility. *Current Research in Food Science, 5*, 288–297. https://doi.org/10.1016/j.crfs.2022.01.019

Žilić, S., Barać, M., Pešić, M., Dodig, D., & Ignjatović-Micić, D. (2011). Characterization of proteins from grain of different bread and durum wheat genotypes. *International Journal of Molecular Sciences, 12*(9), 5878–5894. https://doi.org/10.3390/ijms12095878

Web References

Precedence Research. (2022). *Natural Extracts Market*. Retrieved from https://www.precedenceresearch.com/natural-extracts-market. Accessed November 3, 2022.